Molecular Biology of the Cell
Vol. 10, 4135–4147, December 1999

Luminal Heterodimeric Amino Acid Transporter Defective in Cystinuria

Rahel Pfeiffer,* Jan Loffing,† Grégoire Rossier,‡ Christian Bauch,* Christian Meier,* Thomas Eggermann,§ Dominique Loffing-Cueni,† Lukas C. Kühn,‡ and François Verrey*‖

Institutes of *Physiology and †Anatomy, University of Zürich, CH-8057 Zürich, Switzerland; ‡Swiss Institute for Experimental Cancer Research, CH-1066 Epalinges, Switzerland; and §Institute for Human Genetics, University Hospital of the Rheinisch-Westfälische Technische Hochschule, D-52074 Aachen, Germany

Submitted July 19, 1999; Accepted September 17, 1999
Monitoring Editor: Guido Guidotti

Mutations of the glycoprotein rBAT cause cystinuria type I, an autosomal recessive failure of dibasic amino acid transport ($b^{0,+}$ type) across luminal membranes of intestine and kidney cells. Here we identify the permease-like protein $b^{0,+}$AT as the catalytic subunit that associates by a disulfide bond with rBAT to form a hetero-oligomeric $b^{0,+}$ amino acid transporter complex. We demonstrate its $b^{0,+}$-type amino acid transport kinetics using a heterodimeric fusion construct and show its luminal brush border localization in kidney proximal tubule. These biochemical, transport, and localization characteristics as well as the chromosomal localization on 19q support the notion that the $b^{0,+}$AT protein is the product of the gene defective in non-type I cystinuria.

INTRODUCTION

The membrane glycoprotein rBAT (NBAT, D2) is related to the surface antigen 4F2hc/CD98. These proteins have a similar predicted membrane topology, with a single transmembrane domain and an intracellular NH_2 terminus (type II membrane protein) (Bertran *et al.*, 1992; Tate *et al.*, 1992; Wells and Hediger, 1992). However, in the case of rBAT, an alternative four-transmembrane domain topology has also been proposed (Mosckovitz *et al.*, 1994). When expressed alone in *Xenopus laevis* oocytes, rBAT produces a large amino acid transport, despite the fact that its structure does not resemble that of a transport protein. The induced transport system functions independent of Na^+ and accepts cationic and zwitterionic dibasic amino acids (such as L-arginine, L-lysine, and L-cystine) with high affinity and, with a lower affinity, also zwitterionic (mono)amino acids (such as L-leucine, L-phenylalanine, and L-glutamine). These characteristics correspond to the $b^{0,+}$ system first described in blastocysts, with the difference that rBAT also induces transport of L-cystine (Van Winkle, 1988). Extensive functional studies have shown that the $b^{0,+}$ transport induced by rBAT expression in oocytes (also named $b^{0,+}$-like transport) corresponds to an obligatory exchange of amino acids (Busch *et al.*, 1994; Coady *et al.*, 1994; Chillaron *et al.*, 1996). The electrogenic uptake of cationic amino acids in exchange for neutral amino acids is stimulated by the membrane potential, and the uptake of L-cystine in exchange for monoamino acids is favored by the high concentration gradient maintained by the intracellular reduction of L-cystine to L-cysteine.

The glycoprotein rBAT has been shown to localize to the brush border membranes of kidney straight proximal tubule (S3 segment) (Kanai *et al.*, 1992; Furriols *et al.*, 1993) and small intestine, which are the sites of high-affinity L-cystine (re)absorption, a transport that can be competed by cationic amino acids (Foreman *et al.*, 1980; Schafer and Watkins, 1984; Silbernagl, 1988; Riahi-Esfahani *et al.*, 1995; Palacin *et al.*, 1998). Mutations in the rBAT gene SLC3A1 have been shown to cause at least a large fraction of the cases of the human genetic disease cystinuria type I (OMIM 220100) (Calonge *et al.*, 1994). This inherited malabsorption of L-cystine and dibasic amino acids across renal and intestinal epithelia leads to a severe kidney stone disease (Palacin *et al.*, 1998, and references therein). Non-type I cystinuria (clinically divided in types II and III) differs from type I cystinuria in that heterozygotes have a larger amino aciduria than normals and type I heterozygotes (Rosenberg *et al.*, 1966; Pras *et al.*, 1998). Intestinal malabsorption is less severe in type III than in the other types. The locus of cystinuria type III has been mapped by linkage analysis to chromosome 19q13.1 (Bisceglia *et al.*, 1997; Wartenfeld *et al.*, 1997).

The apically restricted glycoprotein rBAT has been detected by SDS-PAGE analysis as a disulfide-linked oligomer of ~130 kDa composed of an ~85-kDa heavy chain (rBAT) and a second 40–50-kDa protein (light chain) in kidney cortex, jejunum, and rBAT-expressing *Xenopus* oocytes

‖ Corresponding author. E-mail address: verrey@physiol.unizh.ch.

(Wang and Tate, 1995; Palacin *et al.*, 1998). This is similar to the pattern obtained for the glycoprotein 4F2hc, which, in contrast to rBAT, is restricted to the basolateral membrane when expressed in epithelial cells (Quackenbush *et al.*, 1986; Sordat, personal communication).

We and others have recently identified several amino acid permease-like light chains that need to associate with 4F2hc for surface expression (Kanai *et al.*, 1998; Mannion *et al.*, 1998; Mastroberardino *et al.*, 1998; Torrents *et al.*, 1998; Nakamura *et al.*, 1999; Pfeiffer *et al.*, 1999; Prasad *et al.*, 1999; Rossier *et al.*, 2000). These glycoprotein-associated amino acid transporters (gpaATs) function as amino acid exchangers and display L-type or y^+L-type transport specificities with an epithelial, basolateral localization (y^+LAT1 and LAT2) or a broad distribution (LAT1 [= E16/TA1, AmAT-L-lc] and y^+LAT2) (Mastroberardino *et al.*, 1998; Pfeiffer *et al.*, 1999; Rossier *et al.*, 2000; Sordat, personal communication). These highly lipophilic proteins share a topology prediction of 12 transmembrane domains with an intracellular NH_2 terminus. The conserved cysteine residue that forms the disulfide bond with 4F2hc has been identified in the second putative extracellular loop (Pfeiffer *et al.*, 1998) (see Figure 2E).

We have now identified an additional member of the gpaAT family (mouse and human $b^{0,+}$AT) that specifically associates with luminal rBAT, instead of basolateral 4F2hc, to form the $b^{0,+}$ amino acid transporter complex. We show by in situ hybridization and immunofluorescence the localization of $b^{0,+}$AT in the kidney and by expression studies in *Xenopus* oocytes the transport function of the transporter complex ($b^{0,+}$ATc). Concurrently to our study, the members of the cystinuria consortium have identified in the gene encoding the $b^{0,+}$AT transporter (SLC7A9) several mutations causing non-type I cystinuria (Palacin, personal communication). This latter study verifies at the genetic level that $b^{0,+}$AT is involved in the amino acid transport that is defective in cystinuria, whereas our study confirms biochemically, functionally, and at the level of the localization that the SLC7A9 gene encodes the catalytic subunit of the transporter defective in cystinuria.

MATERIALS AND METHODS

Identification and Cloning of $b^{0,+}$AT cDNAs from Mouse and Human

The cDNA for *m*$b^{0,+}$AT was obtained by the ligation of two mouse expressed sequence tag (EST) cDNAs obtained from the I.M.A.G.E. consortium (accession numbers AA273998 and AA105180). Both plasmids were digested with *Bgl*II and *Not*I, and a 400-base pair (bp) fragment of the AA105180 cDNA corresponding to the 3′ end of the mRNA was isolated and cloned into the corresponding sites of AA273998. The *m*$b^{0,+}$AT cDNA coding sequence was subcloned in the vector pSD5easy (Puoti *et al.*, 1997). The cDNA representing an 850-bp 3′ fragment of *h*$b^{0,+}$AT was obtained from the I.M.A.G.E. consortium (accession number R07056). The full-length clone of *h*$b^{0,+}$AT was obtained using Marathon-Ready kidney cDNA (Clontech Laboratories, Palo Alto, CA) as template for 5′ rapid amplification of cDNA ends PCR. The reaction was set up according to the manufacturer's protocol using adaptor primer 1, the gene-specific primer 5′-GGAACGATCCAAGAAGCAGGATAGAG-3′, and the Advantage-HF polymerase kit (Clontech Laboratories). The cycling parameters were as follows: 1 min at 94°C, 5 cycles of 30 s at 94°C/30 s at 68°C/3.5 min at 72°C, 5 cycles of 30 s at 94°C/30 s at 68°C/3.5 min at 70°C, and 25 cycles of 30 s at 94°C/4 min at 68°C. A 1017-bp fragment was recovered by gel extraction, cloned in a TA-type cloning vector (TOPO TA cloning kit, Invitrogen, Carlsbad, CA), and sequenced on both strands (Microsynth, Balgach, Switzerland). The 5′ fragment was ligated to the 3′ EST fragment in the cloning vector pT7T3pac using the restriction sites *Bam*HI in the overlapping sequence and *Eco*RI in the polylinker.

Construction of the hrBAT-m$b^{0,+}$AT Fusion Protein

The linker oligonucleotide encoding the amino acid sequence GAAPDGAPGC was introduced at the 3′ end of the *m*$b^{0,+}$AT cDNA coding sequence starting just before the stop codon by PCR. An amplicon was generated using a sense primer corresponding to the SP6 promoter 5′ of the *m*$b^{0,+}$AT cDNA and a reverse primer corresponding to the end of the coding sequence extended at its 5′ end by the linker sequence and an *Nsi*I restriction site with an in-frame ATG codon (5′-TTGAATGCATCCAGGAGCACCATCAGGAGCAGCACCCTCTGGGTCCTTTTCTGGTGGGAC-3′). The cDNA fragment encoding $b^{0,+}$AT and the linker sequence was isolated after cutting its ends with *Xho*I and *Nsi*I. An *Nsi*I restriction site was introduced in *h*rBAT at the level of the ATG start codon by modifying the two preceding nucleotides (GA→TG) using the QuickChange site-directed mutagenesis kit (Stratagene, La Jolla, CA). The primer sequences were 5′-GAAGACATAAGTCGGTGATGCATGGCTGAAGATAAAAGC-3′ and the corresponding antisense sequence. The $b^{0,+}$AT-encoding fragment was introduced into the vector containing *h*rBAT previously linearized using *Sal*I (compatible with *Xho*I) and *Nsi*I.

FLAG Epitope at the COOH Terminus of hrBAT

A FLAG epitope (DYKDDDDK) was added to the COOH terminus of *h*rBAT (Bertran *et al.*, 1992) using the QuickChange site-directed mutagenesis kit (Stratagene). Briefly, the entire plasmid DNA was amplified using primers each containing a 5′ extension coding for half of the added epitope (5′-GTCCTTGTAGTCACACGAGGTATACAGTATGTTCAGT-3′ and 5′-GACGATGACAAGTAGGCACCTTTATGAAGAGATGAAG-3′). The product was circularized by ligation and used for *Escherichia coli* transformation. The resulting construct was verified by sequence analysis.

cRNA Synthesis

Plasmids containing the cDNA of *h*rBAT, *h*rBAT-*m*$b^{0,+}$AT fusion protein (both vector pSPORT), *m*$b^{0,+}$AT, and *m*y^+LAT1 (both pSD5easy) were linearized using the restriction sites *Hin*dIII for the plasmid pSPORT and *Pvu*II and *Bgl*II for pSD5easy containing *m*$b^{0,+}$AT and *m*y^+LAT1, respectively. cRNA was synthesized with T7 (pSPORT) and SP6 (pSD5easy) RNA polymerase (Promega, Madison, WI), according to standard protocols.

Amino Acid Uptake in X. laevis Oocytes

The treatment of oocytes and uptake experiments were performed essentially as described previously (Pfeiffer *et al.*, 1999). Oocytes were injected with 0.25–10 ng of cRNA dissolved in 33 nl of water and kept for 2–4 d at 16°C in ND96 buffer. Uptake experiments were performed for 1 min (the linearity of uptake was verified in preliminary time course experiments) in buffer supplemented with amino acid at the indicated concentrations and the corresponding ^{3}H-labeled L-amino acid as tracer (except for [^{14}C]L-cystine and [^{14}C]L-isoleucine). Diamide (10 mM) was added to the buffer for experiments with L-cystine.

Amino Acid Uptake in Mouse M1 Cell Lines

The mouse M1 cell line was transfected with expression constructs for *m*$b^{0,+}$AT, *h*rBAT, both (sequentially), or the fusion protein *h*rBAT-*m*$b^{0,+}$AT and a selective marker. Stable cell lines were isolated

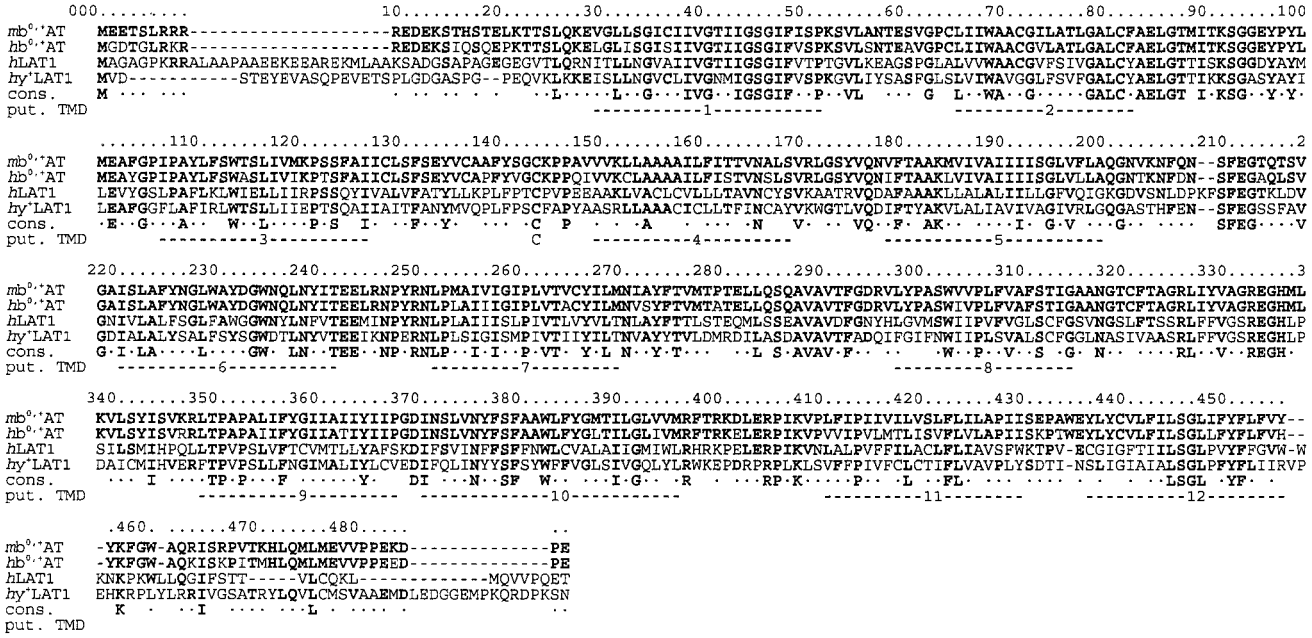

Figure 1. Alignment of mouse and human $b^{0,+}$AT amino acid sequences with *h*LAT1 and *hy*$^+$LAT1. Amino acids identical to those of *mb*$^{0,+}$AT are shown in boldface type. Putative transmembrane domains (TMDs), the positions of which represent compromises based on the predictions obtained for the different sequences (TMpred server, Swiss Institute for Experimental Cancer Research), are numbered from 1 to 12. The conserved cysteine residue known to be involved in the disulfide bond of LAT1 (Pfeiffer *et al.*, 1998) with *h*4F2hc is indicated by the letter C.

by ring cloning or limit dilution (Bauch and Verrey, unpublished data). For uptake experiments, cells were seeded on 3.8-cm^2 cell culture dishes. Before the uptake experiment, cells were washed three times and preincubated for 10 min with buffer containing 150 mM choline-Cl, 5 mM KCl, 1 mM $CaCl_2$, 1 mM $MgCl_2$, 10 mM glucose, 10 mM HEPES, pH 7.4. Then, 80 μl of buffer supplemented with 2.5 μM L-cystine (containing [^{14}C]L-cystine as tracer) and 10 mM diamide was given for 1 min. In control cells, an excess of 200 μM cold L-cystine was added. After removal of the uptake buffer, cells were washed three times and solubilized, and radioactivity was counted by liquid scintillation.

Immunoprecipitation

Oocyte labeling with [^{35}S]methionine for 48 h and lysate preparation were performed as described by Mastroberardino *et al.* (1998). Polyclonal rabbit antibodies were raised against synthetic peptides corresponding to the NH_2 termini of *mb*$^{0,+}$AT and *h*rBAT (number 400, NH_2-MEETSLRRRREDEKSTHC-COOH, and number 563, NH_2-MAEDKSKRDSIEMSMKGC-COOH, respectively) coupled to keyhole limpet hemocyanin (Eurogentec, Seraing, Belgium) and were used, along with a polyclonal anti-FLAG antibody (Santa Cruz Biotechnology, Santa Cruz, CA), for immunoprecipitations. Antibodies were prebound to protein G plus protein A–agarose (Calbiochem, La Jolla, CA) for 2 h at room temperature. The beads were then added to lysate (each sample containing the same amount of incorporated radioactive methionine) that had been precleared by two incubations with uncoated beads. For precipitation with anti-FLAG antibody, the lysate was first treated with 3% SDS and 5 min of boiling and diluted 10-fold with buffer containing 1% NP40. The beads were rotated overnight at 4°C and then washed. The precipitate was eluted in SDS-PAGE sample buffer and heated to 65°C for 15 min. β-Mercaptoethanol was added where indicated, and SDS-PAGE analysis was performed. Gels were stained in Coomassie blue, fixed, incubated in Amplify (Amersham, Arlington Heights, IL), dried, and exposed to film.

Northern Blot

Total RNA from various tissues of two female and two male (for testes) B10D2 mice (kindly provided by Werner Held, Ludwig Institute for Cancer Research) and a B6D2 mouse (for placenta) (kindly provided by Friedrich Beerman, Swiss Institute for Experimental Cancer Research) was isolated using a cesium chloride method. Fifteen micrograms of total RNA was loaded on a 1.2% agarose/formaldehyde gel, transferred onto GeneScreen Plus membrane (New England Nuclear, Boston, MA), and UV cross-linked. *mb*$^{0,+}$AT (bp 1–515) and *m*rBAT (EST cDNA AA388506, bp 21–363) cDNA fragments were labeled with [α-^{32}P]dCTP by random priming. Hybridized and washed membranes were exposed on Kodak (Rochester, NY) Biomax film.

Tissue Fixation and Processing

Adult male Zur:ICR mice (Institut für Labortierkunde, Zürich, Switzerland) were anesthetized with an intraperitoneal injection of 50 μl of anesthetic solution, and tissues were then fixed and processed as described by Loffing *et al.* (1996).

In Situ Hybridization

A mouse rBAT cDNA fragment was generated by reverse transcriptase PCR using the following primers derived from a published sequence: 5′-AGCACCAGGAAGAGCTACACAGGGT-3′ and 5′-ACGTGCATCGTGCTACAGAAATATCTA-3′. This fragment was subcloned in pSPORT1. Digoxigenin-11-UTP–labeled riboprobes for mouse rBAT and $b^{0,+}$AT were synthesized by in vitro transcription (DIG RNA labeling kit [Sp6/T7], Boehringer Mannheim [Indianap-

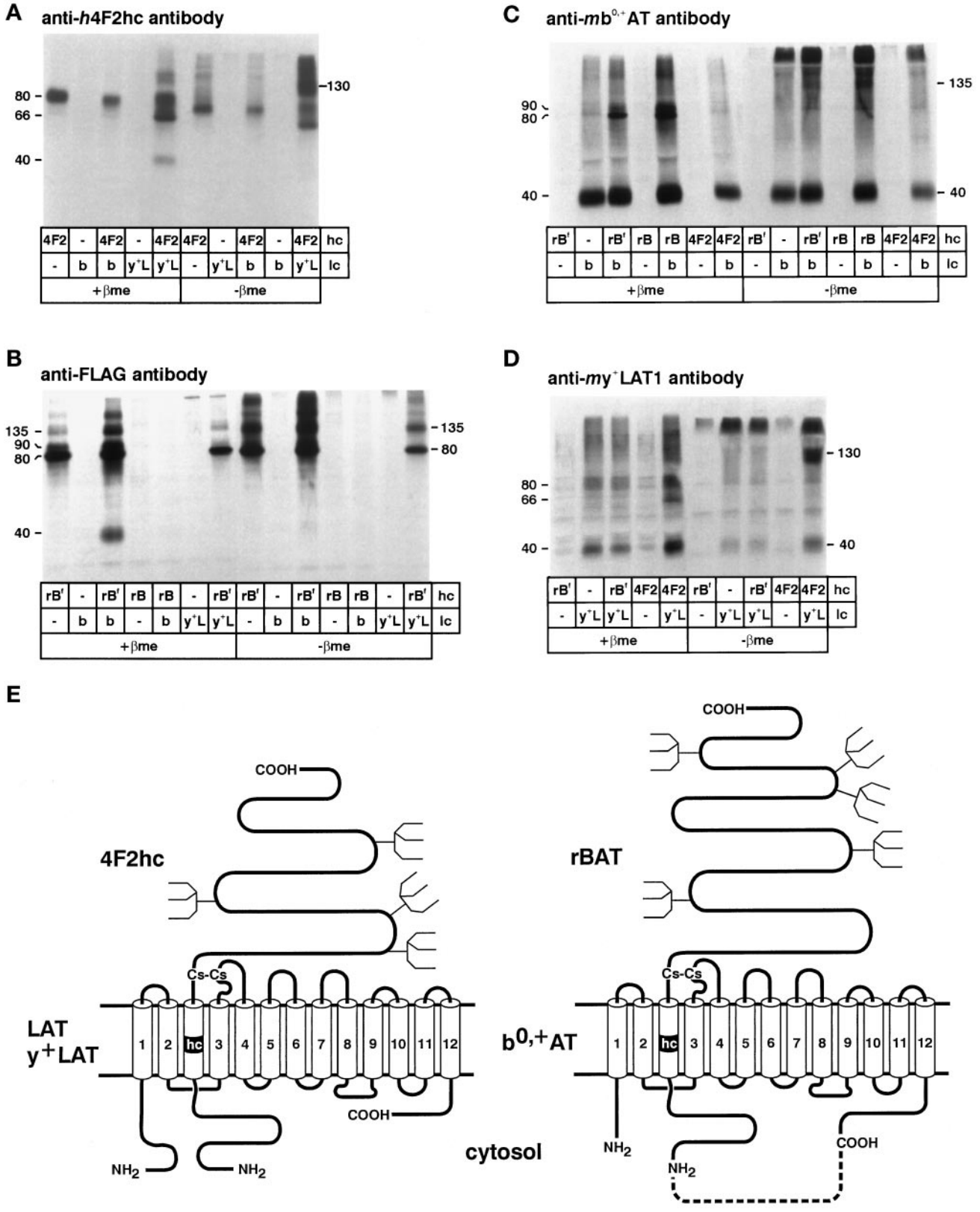
A
anti-h4F2hc antibody
80
66
40
130
4F2 - 4F2 - 4F2 4F2 - 4F2 - 4F2 hc
- b b y+L y+L - y+L b b y+L lc
+βme -βme
C
anti-mb0,+AT antibody
90
80
40
135
40
rB' - rB' rB rB 4F2 4F2 rB' - rB' rB rB 4F2 4F2 hc
- b b - b - b - b b - b - b lc
+βme -βme
B
anti-FLAG antibody
135
90
80
40
135
80
rB' - rB' rB rB - rB' rB' - rB' rB rB - rB' hc
- b b - b y+L y+L - b b - b y+L y+L lc
+βme -βme
D
anti-my+LAT1 antibody
80
66
40
130
40
rB' - rB' 4F2 4F2 rB' - rB' 4F2 4F2 hc
- y+L y+L - y+L - y+L y+L - y+L lc
+βme -βme
E
COOH
4F2hc
Cs-Cs
LAT
y+LAT
1 2 hc 3 4 5 6 7 8 9 10 11 12
COOH
NH2
NH2
COOH
rBAT
Cs-Cs
b0,+AT
1 2 hc 3 4 5 6 7 8 9 10 11 12
NH2
NH2
COOH
cytosol

Figure 2.

olis, IN]). Plasmids containing either mouse rBAT cDNA or $b^{0,+}$AT cDNA were linearized using the appropriate restriction enzymes Antisense probes for mouse rBAT and $b^{0,+}$AT were generated by T7 RNA polymerase and T3 RNA polymerase, respectively. For control, sense riboprobes for mouse rBAT and $b^{0,+}$AT were transcribed by Sp6 RNA polymerase and T7 RNA polymerase, respectively. RNA probes were shortened by alkaline hydrolysis to fragments of an average length of ~200 bp.

Cryostat sections (7 μm thick) were postfixed with 4% paraformaldehyde/PBS for 20 min at room temperature. The slides were then rinsed with diethylpyrocarbonate-treated water followed by two short washes in PBS. The cryosections were pretreated for 10 min with proteinase K (5 μg/ml; Sigma, St. Louis, MO) and 0.025% collagenase type 5 (Sigma) at room temperature followed by two short rinses in PBS. Acetylation (0.1 M triethanolamine and 0.25% acetic anhydrate) was performed for 20 min at room temperature. After two short rinses in PBS, sections were dehydrated in ethanol (70, 80, and 100%) and air dried for 20 min. Prehybridization was performed at 42°C for 2 h (50% formamide, 50 mM Tris-HCl, pH 7.6, 25 mM EDTA, pH 8, 20 mM NaCl, 0.2% SDS, 2.5× Denhardt's solution, 0.25 mg/ml tRNA). Hybridization was performed at 42°C for 16–18 h (50% formamide, 20 mM Tris-HCl, pH 7.6, 1 mM EDTA, pH 8, 33 mM NaCl, 10 mM DTT, 0.5 mg/ml tRNA, 0.1 mg/ml DNA, 1× Denhardt's solution, 12.5% dextran sulfate; optimal concentration of digoxigenin-labeled riboprobes was 8 ng/μl of hybridization mixture).

Slides were washed once with 2× SSC (SSC = 150 mM NaCl, 15 mM Na citrate) at room temperature for 15 min followed by three sequential washes at 49°C each for 1 h in 1× SSC/50% formamide followed by 0.5× SSC/50% formamide and 0.2× SSC/50% formamide. This treatment was followed by two short rinsing steps in 0.5× SSC and 0.2× SSC. Digoxigenin-labeled probes were detected with the DIG RNA detection kit (Boehringer Mannheim) according to the manufacturer's instructions. The provided alkaline phosphatase–linked sheep anti-digoxigenin antibody was diluted 1:500. Nitroblue tetrazolium salt and 5-bromo-4-chloro-3-indolyl phosphate served as chromogenic substrates for the alkaline phosphatase–catalyzed color reaction. Endogenous activity of alkaline phosphatase was blocked by the addition of 5 mM levamisole (Sigma) to the substrate solution.

Immunohistochemistry

Serial sections (4 μm thick) were cut in a cryostat and placed on chrome-alum-gelatin–coated glass slides. After preincubation of the sections with 10% normal goat serum (DAKO, Glostrup, Denmark), the sections were incubated overnight at 4°C with a 1:500 dilution of antiserum 400, which was raised against a NH_2-terminal peptide of $b^{0,+}$AT (see above). After repeated washing with PBS, the binding sites of the primary antibody were revealed with a Cy3-conjugated donkey anti-rabbit immunoglobulin G (Jackson Immunoresearch, West Grove, PA) diluted 1:1000. Subsequently, sections were washed in PBS, mounted in DAKO-glycergel (DAKO) containing 2.5% 1,4-diazabicyclo [2,2,2]octane as fading retardant, and studied by epifluorescence with a Polyvar microscope (Reichert Jung, Vienna, Austria). For controls, consecutive cryosections were incubated with either preimmune serum or the anti-$b^{0,+}$AT antiserum preabsorbed for 1 h with the corresponding antigenic peptide (20 μg/ml). Digitized images were acquired with a VISICAM charge-coupled device camera (Visitron, Puchheim, Germany) attached to the microscope and processed by Image-Pro Plus version 3.0 software (Media Cybernetics, Silver Spring, MD).

Fluorescent In Situ Hybridization

The cDNA *h*$b^{0,+}$AT was labeled with Biotin-11-dUTP in a nick translation reaction (GIBCO-BRL, Gaithersburg, MD), and 1 μg was precipitated with 10 μg of salmon sperm DNA and 100 μg of cot1 DNA, dissolved in hybridization buffer (50% deionized formamide, 10% dextran sulfate, 2× SSC), and denatured at 75°C for 5 min. Metaphase spreads were prepared from human peripheral blood lymphocyte cultures by standard procedures, and the chromosomal DNA was denatured for 3 min at 75°C in buffer containing 70% formamide and 2× SSC, pH 7.0. After passing the denatured spreads through an ice-cold ethanol series (70%, 90%, and absolute for 3 min each, air drying), probe was dropped onto them, covered with an 18- × 18-mm coverslip, sealed with rubber cement, and incubated at 37°C for 12 h. High-stringency washes were performed three times for 5 min in 50% formamide/2× SSC at 45°C and in 0.1× SSC at 60°C, followed by a final wash of 5 min in 4× SSC/0.05% Tween 20 at room temperature. Hybridization signals were revealed using avidin-FITC (Vector Laboratories, Burlingame, CA), and chromosomes were counterstained with DAPI.

Data Bank Accession Numbers

Accession numbers are as follows: *m*$b^{0,+}$AT, AJ249198; *h*$b^{0,+}$AT, AJ249199.

RESULTS

Recently, LAT1 and y^+LAT1 have been identified as light chains of the type II glycoprotein 4F2hc (Kanai *et al.*, 1998; Mastroberardino *et al.*, 1998; Torrents *et al.*, 1998; Pfeiffer *et al.*, 1999), a surface protein with a high level of structural

Figure 2 (facing page). Selective coimmunoprecipitation of *m*$b^{0,+}$AT with *h*rBAT (or *h*$rBAT^{FLAG}$) and of *m*y^+LAT1 with *h*4F2hc. Oocytes were injected with cRNA for a heavy chain (hc) (rB^f = *h*$rBAT^{FLAG}$; rB = *h*rBAT; 4F2 = *h*4F2hc) and/or a light chain (lc) (b = *m*$b^{0,+}$AT; y^+L = *m*y^+LAT1) as indicated. (A) From oocytes expressing *h*4F2hc alone, anti-*h*4F2hc antibody precipitated a protein migrating as two bands of ~66 and ~80 kDa that correspond to the core- and terminally glycosylated forms of *h*4F2hc. As expected, coexpressed *m*y^+LAT1 was coprecipitated with *h*4F2hc and migrated as an additional band of ~40 kDa when the sample was treated with the reducing agent β-mercaptoethanol (β-me) and as a heterodimeric complex of ~130 kDa in its absence. In contrast, there was no coprecipitation of *m*$b^{0,+}$AT with *h*4F2hc. (B) Anti-FLAG antibody precipitated a protein migrating as two bands of ~80 and ~90 kDa that presumably represent the core-glycosylated and the terminally glycosylated forms of *h*$rBAT^{FLAG}$. When the oocytes coexpressed *m*$b^{0,+}$AT with *h*$rBAT^{FLAG}$, an additional band of ~40 kDa was coprecipitated. In nondenaturing conditions, the proteins remained assembled mainly as heterodimers and migrated at a level of ~135 kDa. *m*y^+LAT1 was not coprecipitated with $rBAT^{FLAG}$. (C) *m*$b^{0,+}$AT was immunoprecipitated by anti-*m*$b^{0,+}$AT antibody (~40 kDa), and *h*rBAT and *h*$rBAT^{FLAG}$ were coprecipitated and appear as additional bands of ~80 and ~90 kDa (compare with B). *h*4F2hc was not coprecipitated with *m*$b^{0,+}$AT. (D) *m*y^+LAT1 was immunoprecipitated by anti-*m*y^+LAT1 antibody (~40 kDa), and additional bands of ~80 and ~90 kDa corresponding to coprecipitated *h*4F2hc appeared when *h*4F2hc was coexpressed (compare with A). *h*rBAT was not coprecipitated with *m*y^+LAT1. (E) Scheme of the heterodimers formed by the heavy chain 4F2hc with LAT or y^+LAT light chains and of the heterodimers formed by rBAT with $b^{0,+}$AT. The single evident transmembrane domain of the heavy chains is labeled hc, and the 12 putative transmembrane domains of the lipophilic light chain are numbered 1–12. The dotted line between the COOH terminus of $b^{0,+}$AT and the NH_2 terminus of rBAT represents the linker sequence introduced to form a functional fusion protein. The localization of the conserved cysteine residues forming the intermolecular disulfide bond has been demonstrated for the heavy chain 4F2hc and the light chains *Xenopus* LAT1 (ASUR4) and *Schistosoma mansoni* SPRM1 (Pfeiffer *et al.*, 1998). Potential *N*-glycosylation sites are indicated by forks.

similarity to rBAT (Bertran *et al.*, 1992; Tate *et al.*, 1992; Wells and Hediger, 1992). Performing database searches (BLAST programs, National Center for Biotechnology Information) with the sequences of *h*LAT1 and *m*y$^+$LAT1, we identified two overlapping mouse EST sequences that together form a cDNA encoding a full-length 487-amino acid protein (*m*b$^{0,+}$AT) that is equally similar to human LAT1 and y$^+$LAT1 (44% identity on 483–486 aligned amino acids; ToPLign Server, Sankt Augustin, Germany) (Figure 1). We further identified an ~850-bp EST cDNA that corresponds to the 3′ end of the human orthologue mRNA. The missing part of the human sequence was obtained by 5′ rapid amplification of cDNA ends PCR. The deduced primary structures from mouse and human b$^{0,+}$AT have the same number of amino acids and are 86.7% identical (Figure 1).

mb$^{0,+}$AT Forms a Covalently Linked Heterodimer with hrBAT

We have previously shown by immunoprecipitation that the surface glycoprotein *h*4F2hc very efficiently covalently binds to at least three different members of the glycoprotein-associated amino acid transporter family, LAT1, LAT2 (Rossier *et al.*, 2000), and y$^+$LAT1, as demonstrated by coimmunoprecipitation of proteins coexpressed in *Xenopus* oocytes. Figure 2A shows that, in contrast, *m*b$^{0,+}$AT did not bind to *h*4F2hc. Indeed, as expected, immunoprecipitation of *h*4F2hc yielded a band migrating at the level of ~80 kDa on SDS-PAGE (core glycosylated form, ~66 kDa), and coexpressed *m*y$^+$LAT1 was coprecipitated and migrated as an ~40-kDa band when the samples were reduced (Mastroberardino *et al.*, 1998; Pfeiffer *et al.*, 1998, 1999). Coexpression of y$^+$LAT strongly increased the proportion of the core-glycosylated form of 4F2hc that migrated at 66 kDa, as discussed previously (Pfeiffer *et al.*, 1999). When reduction was omitted, the heterodimer formed by *h*4F2hc and *m*y$^+$LAT1 migrated as an ~130-kDa complex (some complex was also visible after reduction). In contrast, no coprecipitated light chain was observed when *h*4F2hc was coexpressed with *m*b$^{0,+}$AT, showing that y$^+$LAT1 but not b$^{0,+}$AT heterodimerizes with 4F2hc.

To test the hypothesis that b$^{0,+}$AT heterodimerizes with rBAT, the 4F2hc-related apical protein known to be defective in many cases of cystinuria type I, coexpression experiments of *m*b$^{0,+}$AT and *h*rBAT (extended at the COOH terminus by a FLAG epitope [*h*rBAT^{FLAG}]) were performed (Figure 2B). The anti-FLAG antibody was shown to be specific, because it immunoprecipitated *h*rBAT^{FLAG} (doublet of ~80 and ~90 kDa corresponding most probably to core-glycosylated and terminally glycosylated forms, respectively) but not *h*rBAT without FLAG, *h*4F2hc, or any of the light chains expressed alone. Coexpression of *h*rBAT^{FLAG} with *m*b$^{0,+}$AT but not *m*y$^+$LAT1 led to the appearance of an additional band of ~40 kDa under reducing conditions, corresponding to coprecipitated *m*b$^{0,+}$AT. Under nonreducing conditions, the complex remained associated and migrated as a major heterodimeric complex of ~135 kDa and as higher-molecular-mass bands corresponding possibly to higher-order complexes. The same pattern was obtained using anti-*h*rBAT antibody (data not shown). These results indicate that *h*rBAT and *m*b$^{0,+}$AT are covalently linked by a disulfide bond, similar to the association of the other light chains with 4F2hc. A band at the same level (~135 kDa) was also apparent when *h*rBAT^{FLAG} was expressed alone or in the presence of *m*y$^+$LAT1. This band is slightly weaker and corresponds most probably to the heterodimeric complex formed by *h*rBAT^{FLAG} and an endogenous oocyte light chain (Wang and Tate, 1995; Palacin *et al.*, 1996). The fact that this putative endogenous light chain is hardly visible when the complex is dissociated by reduction indicates that it is only weakly labeled by the pulse-labeling procedure and thus that most of this endogenous protein must preexist the expression of exogenous rBAT. This situation is analogous to that of the Na,K-ATPase α subunit of *Xenopus* oocytes, which is present in large excess over the endogenous β subunit and can be activated by expressing exogenous β subunit (Geering *et al.*, 1989).

Similar experiments were also performed with antibodies recognizing the light chains (Figure 2, C and D). Immunoprecipitation with anti-*m*b$^{0,+}$AT antibody (Figure 2C) yielded the expected band of ~40 kDa for *m*b$^{0,+}$AT. Efficient coprecipitation of *h*rBAT and *h*rBAT^{FLAG} (80- and 90-kDa bands, respectively, after reduction) but not of *h*4F2hc was observed. In nonreducing conditions, an ~135-kDa band that probably represents a heterodimer of *m*b$^{0,+}$AT and *h*rBAT was visible only when *h*rBAT was coexpressed with *m*b$^{0,+}$AT. In contrast, a high-molecular-mass aggregate, the nature of which is not known, also was visible in the absence of *h*rBAT. Figure 2D shows that anti-*m*y$^+$LAT1 antibody coprecipitates *h*4F2hc (~66- and 80-kDa bands in reducing conditions and an ~130-kDa band [heterodimer] in nonreducing conditions) with *m*y$^+$LAT but not *h*rBAT or *h*rBAT^{FLAG} (Pfeiffer *et al.*, 1999). These results demonstrate that *m*b$^{0,+}$AT heterodimerizes with *h*rBAT but not with *h*4F2hc, in contrast to *m*y$^+$LAT1, which associates with *h*4F2hc but not with *h*rBAT. Figure 2E shows a scheme of the heterodimers formed by 4F2hc with LAT or y$^+$LAT light chains and of those formed by rBAT with b$^{0,+}$AT. The cytosolic localization of the light chain COOH terminus is confirmed by the expression of a functional fusion protein when b$^{0,+}$AT and rBAT are fused by a 10-amino acid linker sequence (dotted line; see below).

Transport Properties of mb$^{0,+}$AT

To test whether b$^{0,+}$AT functions as an amino acid transporter, we measured the uptake of radioactively labeled L-arginine in water-injected oocytes and oocytes expressing *m*b$^{0,+}$AT (Figure 3A). No uptake of L-arginine over background levels was observed in oocytes expressing *m*b$^{0,+}$AT alone. As expected, *h*rBAT induced an efficient uptake of L-arginine, and coexpression of *m*b$^{0,+}$AT did not further increase the uptake of L-arginine. This is compatible with the hypothesis that *h*rBAT very efficiently associates with an endogenous oocyte transport protein light chain (Wang and Tate, 1995; Palacin *et al.*, 1996) and that much of this light chain preexists *h*rBAT synthesis, as indicated by the result shown in Figure 2B and discussed above.

To prevent expressed *h*rBAT from heterodimerizing with this preexisting endogenous oocyte light chain, we constructed a cDNA encoding a fusion protein in which *h*rBAT was linked by its NH_2 terminus to the COOH terminus of *m*b$^{0,+}$AT. A linker sequence of 10 amino acids was introduced between the two protein moieties (see scheme in Figure 2E). This sequence was designed to contain, besides a negative charge, several alanine and proline residues (Mao

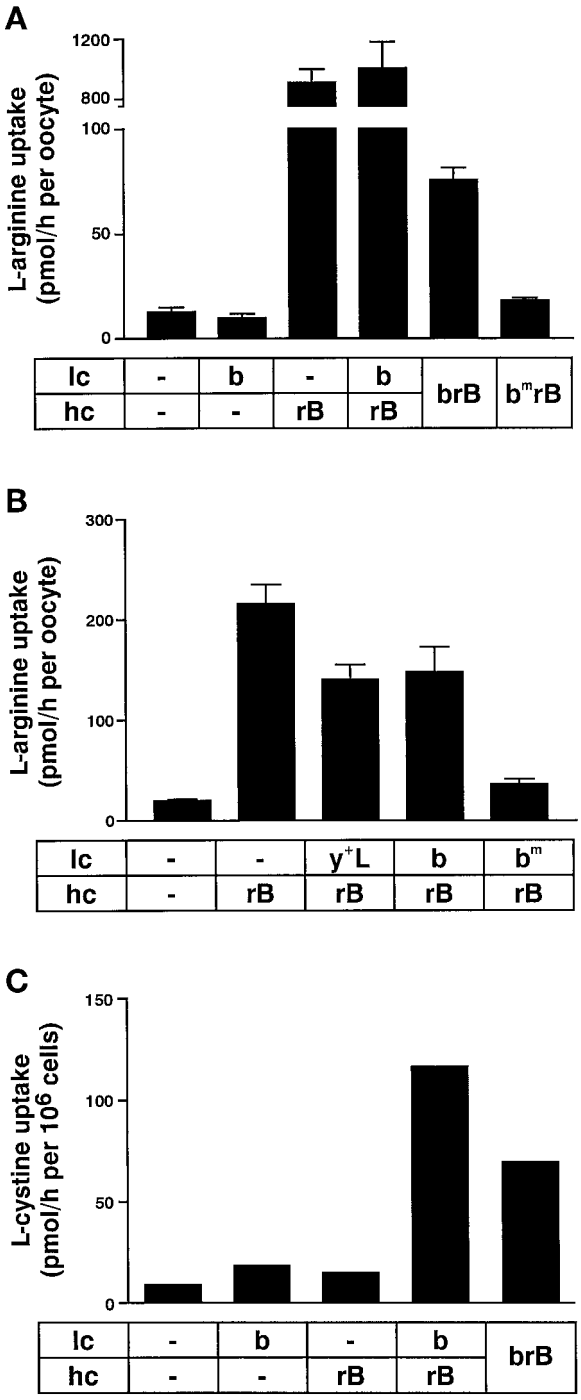

Figure 3. Both *h*rBAT and *m*b$^{0,+}$AT are required for the expression of b$^{0,+}$-type transport function. (A) No L-arginine uptake over background level was observed when oocytes expressed the b$^{0,+}$AT light chain (b) alone. *h*rBAT (rB) alone, which associated with endogenous oocyte light chains, induced a high transport rate. Coexpression of the b$^{0,+}$AT light chain with rBAT did not modify the transport rate significantly. The fusion protein *h*rBAT-*m*b$^{0,+}$AT (brB) induced in oocytes an L-arginine uptake that was severalfold higher than that observed with fusion protein containing the mutant b$^{0,+}$AT^{E244Q} light chain moiety (b^{m}rB) or that of water-injected oocytes. (B) Oocytes were first injected with the light chain cRNA for *m*b$^{0,+}$AT, *m*b$^{0,+}$AT^{E244Q}, or *my*$^{+}$LAT. After 2 d of expression, *h*rBAT cRNA was injected and L-arginine uptake was measured 24 h later. The preexpression of the mutant light chain *m*b$^{0,+}$AT^{E244Q} nearly fully inhibited L-arginine uptake expression induced by rBAT, presumably by efficiently competing with functional endogenous chains for association with rBAT. Means of 12 oocytes ± SEM are shown. (C) Mouse M1 cell lines expressing rBAT, b$^{0,+}$AT, both, or the fusion protein *h*rBAT-*m*b$^{0,+}$AT (brB) were seeded on plastic dishes, and the uptake of L-cystine (2.5 μM) was measured. A single experiment with one cell line each is shown. Several cell lines were tested for single and double transfectants and gave comparable results. Uptakes significantly higher than by untransfected control cells were obtained only in double transfectant and fusion protein–expressing cell lines (Bauch and Verrey, unpublished data).

et al., 1995). Although L-arginine uptake by oocytes expressing this fusion protein was lower than in *h*rBAT-expressing oocytes, there was a threefold to sixfold induction of amino acid transport over background levels. In contrast, when the conserved residue Glu-244 of the *m*b$^{0,+}$AT moiety of the fusion protein was mutated to Gln (located in the putative intracellular loop between transmembrane domains 6 and 7), L-arginine uptake was completely abolished. This shows that amino acid transport is mediated by the fused b$^{0,+}$AT light chain and not by an associated oocyte light chain. This point mutation in b$^{0,+}$AT was chosen based on preliminary tests made with SPRM1, a *Schistosoma mansoni* member of the gpaAT family that heterodimerizes with 4F2hc (Mastroberardino *et al.*, 1998). In this light chain, the equivalent mutation (E237Q) was shown to completely abolish transport function, whereas the cell surface expression was identical to that of wild-type SPRM1 (Mastroberardino *et al.*, 1998) (data not shown).

To functionally confirm that in oocytes rBAT can associate with either endogenous light chain and/or with coexpressed b$^{0,+}$AT light chain, the b$^{0,+}$ transport function was measured after injection of different exogenous light chains potentially competing with the endogenous one for binding to rBAT (Figure 3B). The biosynthetic apparatus of oocytes was prefilled with various exogenous light chains by first injecting a large amount of their cRNAs (10 ng). These preinjected light chains were wild-type *m*b$^{0,+}$AT, shown above to bind rBAT and which presumably is functional, mutant *m*b$^{0,+}$AT, which binds to rBAT but is not functional, and *my*$^{+}$LAT1, which does not bind to rBAT and thus is not expected to compete with endogenous light chains. cRNA of *h*rBAT (2.5 ng) was injected 2 d after the light chain cRNA, and L-arginine uptake experiments were performed 1 d later. In these conditions, *my*$^{+}$LAT1 and *m*b$^{0,+}$AT preexpression slightly decreased L-arginine uptake compared with control oocytes preinjected with water only, probably because of competition at the level of the translation machinery of the large amount of preinjected cRNA with the postinjected rBAT cRNA. In contrast, L-arginine uptake was completely inhibited by the preexpression of mutant *m*b$^{0,+}$AT. Thus, in the presence of high amounts of exogenous mutant *m*b$^{0,+}$AT light chain, *h*rBAT no longer efficiently binds to endogenous light chain. This strongly suggests that in the case of preexpression of wild-type *m*b$^{0,+}$AT, *h*rBAT similarly associates mainly with this exogenous light chain and thus the measured transport is mediated by the complex *h*rBAT-*m*b$^{0,+}$AT.

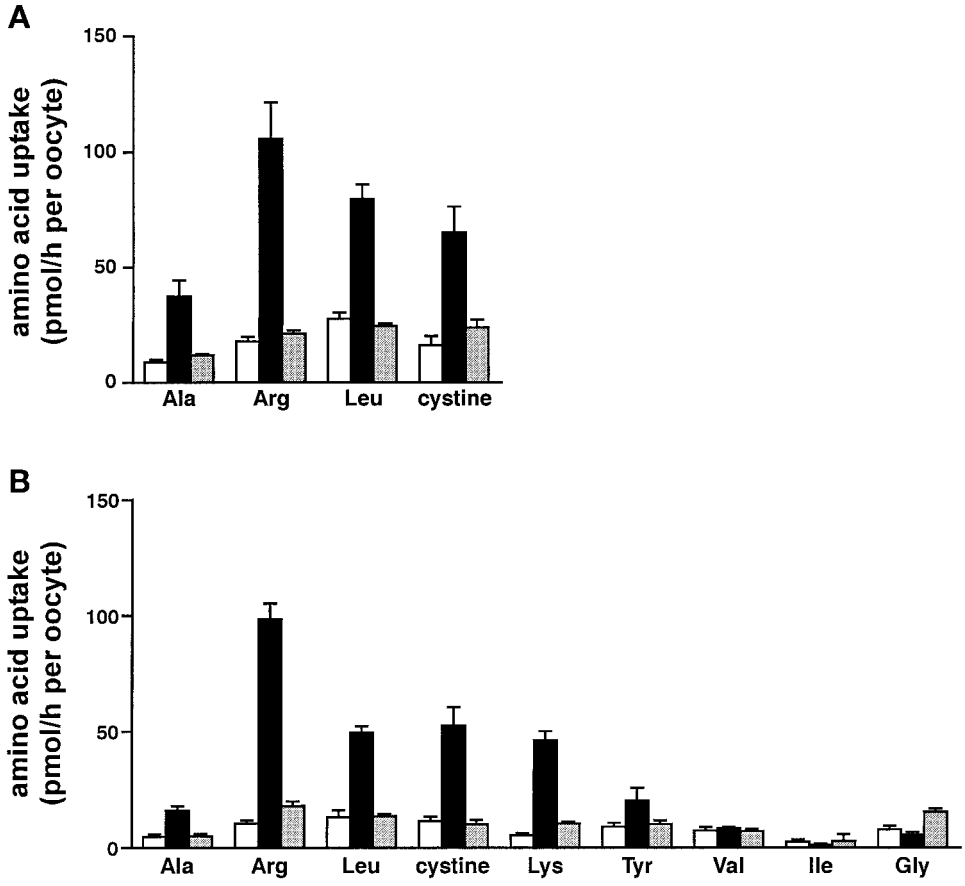

Figure 4. Specificity of amino acid uptake by oocytes expressing the *m*rBAT-$b^{0,+}$AT fusion protein. The tested amino acids were given for 1 min at a concentration of 100 μM in the presence (A) or absence (B) of Na^+. The black bars represent the test values for oocytes expressing the fusion protein *m*rBAT-$b^{0,+}$AT. Oocytes injected with water (white bars) or the mutant fusion protein *h*rBAT-*m*$b^{0,+}AT^{E244Q}$ (gray bars) represent controls. Means of 12 oocytes ± SEM pooled from two independent experiments are shown.

To verify in cells expressing no endogenous $b^{0,+}$AT light chain that both rBAT and the light chain $b^{0,+}$AT are required to form the functional high-affinity L-cystine transporter, mouse epithelial M1 cell lines expressing either one or both subunits were produced. Figure 3C shows an example of L-cystine (2.5 μM) uptake obtained with one set of cell lines. In none of the cell lines expressing a single subunit was the rate of [^{14}C]L-cystine uptake (inhibited by cold L-cystine) significantly greater than the level measured in untransfected controls. However, a 6- to 40-fold higher transport rate was observed in the cell lines expressing both rBAT and $b^{0,+}$AT. The fact that cell lines expressing the *h*rBAT-*m*$b^{0,+}$AT fusion protein produced L-cystine uptake like those expressing the unlinked subunits supports our conclusion that the transports measured in *Xenopus* oocytes with the same fusion protein are representative of the function of the hetero-oligomeric $b^{0,+}$ATc.

To test the specificity of the transport induced by the rBAT-$b^{0,+}$AT complex in *Xenopus* oocytes, experiments were performed with the fusion protein *h*rBAT-*m*$b^{0,+}$AT. Oocytes were injected with cRNA for the mutant fusion protein *h*rBAT-*m*$b^{0,+}AT^{E244Q}$ or water for controls. The uptake of radioactively labeled amino acids (100 μM) was measured within the linear phase of transport and is given in picomoles per hour (Figure 4). The fusion protein transported, independent of the presence of Na^+, the cationic dibasic amino acids L-arginine and L-lysine, the neutral dibasic L-cystine, and the neutral monoamino acids L-leucine and L-alanine, as expected for $b^{0,+}$-type rBAT-associated amino acid transport. There was little transport of L-tyrosine. The β-branched neutral amino acids L-valine and L-isoleucine as well as L-glycine were not transported significantly in these conditions.

Figure 5 shows the plots of dose-response experiments performed for L-arginine, L-cystine, and L-leucine uptakes. Curves corresponding to Michaelis-Menten kinetics were fitted to the experimental points, and apparent affinity values (K_m) were derived. The K_m values (±SEM) for L-arginine and L-cystine were 72 ± 35 μM and 41 ± 20 μM, respectively. The K_m for L-leucine was much higher (1.1 ± 0.7 mM) and was also higher than previously reported for oocytes injected with rBAT alone. The difference might represent a species variation between the mammalian $b^{0,+}$AT light chain and the endogenous *X. laevis* light chain present in oocytes. The higher affinity of *m*$b^{0,+}$AT toward L-arginine and L-cystine compared with L-leucine might reflect the function of the transporter, which has been shown to preferentially take up dibasic amino acids in exchange for neutral amino acids (Chillaron *et al.*, 1996). Experiments with epithelial cells expressing both subunits of the $b^{0,+}$ATc (see above) show apparent affinities for the uptake of amino acids similar to those measured here for *Xenopus* oocytes expressing the fusion protein *h*rBAT-*m*$b^{0,+}$AT (Bauch and Verrey, unpublished observations).

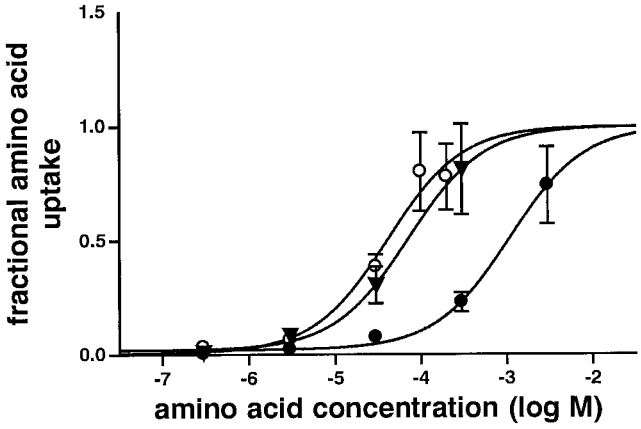

Figure 5. Concentration dependence of L-cystine (○), L-arginine (▼), and L-leucine (●) uptake by oocytes expressing the *h*rBAT-*m*b$^{0,+}$AT fusion protein. Uptake experiments were performed at five or six different amino acid concentrations, and background uptake by water-injected oocytes was subtracted. Sigmoidal curves corresponding to Michaelis-Menten kinetics were fitted to the experimental data using a nonlinear regression routine. For every concentration, data from means of 12 oocytes ± SEM pooled from two independent experiments are shown. The apparent K_m derived from the curves for L-cystine, L-arginine, and L-leucine were 41 μM, 72 μM, and 1.1 mM, respectively.

Preliminary experiments have shown that L-arginine efflux from the oocytes takes place only when the fusion protein *h*rBAT-*m*b$^{0,+}$AT containing the wild-type mb$^{0,+}$AT moiety is expressed and that this efflux is strictly dependent on the presence of an extracellular amino acid (our unpublished results). This confirms results obtained with rBAT expressed alone and thus associated with endogenous oocyte light chain (Busch *et al.*, 1994; Coady *et al.*, 1994; Chillaron *et al.*, 1996).

Common and Differential Localizations of b$^{0,+}$AT and rBAT

Northern blot analysis of mouse tissues shows that a major b$^{0,+}$AT transcript of ~2 kilobase (kb) is expressed specifically in (small) intestine and kidney (Figure 6A). Weaker signals at a higher molecular weight (~4.5 kb and/or ~6 kb) can be seen in most other tested tissues. rBAT data (Figure 6B) are shown for comparison. In this case, the signal of the major transcript (~2.5 kb) also is clearly visible only in kidney and intestine and is slightly visible in liver. A higher-molecular-weight transcript (~4.5 kb) is expressed in brain, as reported previously in other species (Bertran *et al.*, 1992, 1993; Yan *et al.*, 1992).

The localization of rBAT and b$^{0,+}$AT in the kidney was analyzed by in situ hybridization (rBAT and b$^{0,+}$AT) and immunofluorescence (b$^{0,+}$AT) (Figure 7). Panels b and g show that in mice, rBAT mRNA was localized not only to the straight part of the proximal tubules (S3 segments), as reported previously for the protein of rat (Furriols *et al.*, 1993), but also, although at a lower level, to the preceding S1 and S2 segments, as reported previously for the mRNA of rat (Kanai *et al.*, 1992). By contrast, b$^{0,+}$AT mRNA was most highly expressed in the S1 segments (panels c and h) and was only barely detectable in S2 and S3 segments within the medullary rays and outer medulla (panel h). Immunofluorescence confirmed, at the protein level, that b$^{0,+}$AT was highly abundant in S1 (panels d and i) and was present at lower levels in S2 and S3 segments. Staining intensity in S3 segments was consistently lower than that in S2 segments (panels i and k). The immunohistochemistry clearly demonstrated that, at the subcellular level, b$^{0,+}$AT was present in

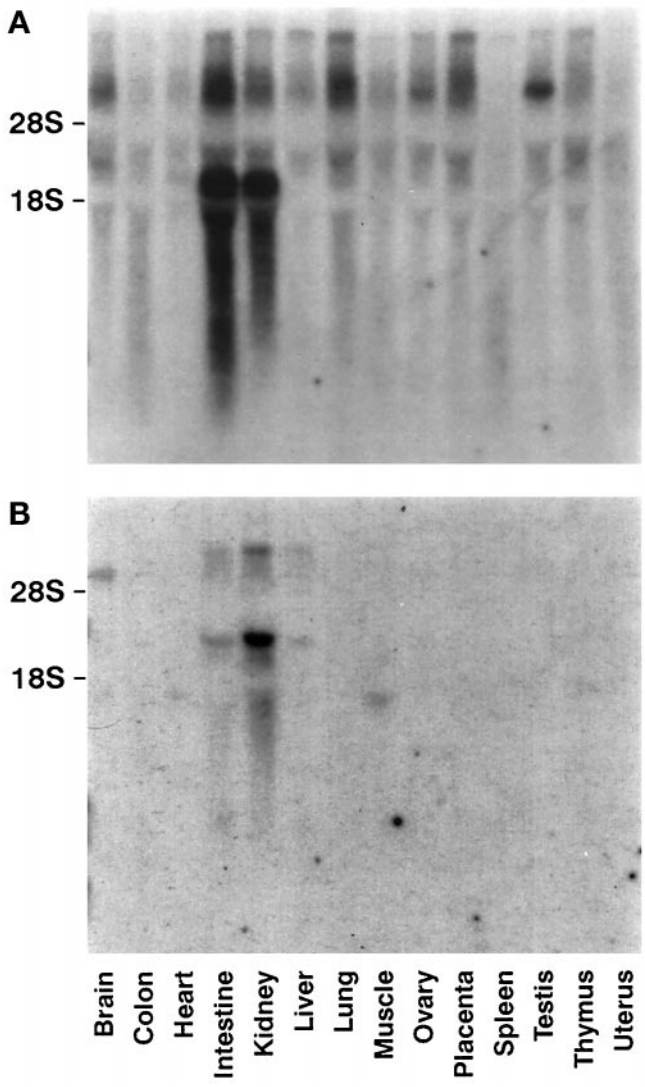

Figure 6. Tissue distribution of rBAT and b$^{0,+}$AT in the mouse. (A) Northern blot analysis of mouse tissue RNAs shows a major b$^{0,+}$AT transcript of ~2 kb specifically expressed in intestine and kidney. Weaker signals at a higher molecular weight (~4.5 kb and/or ~6 kb) can be seen in most other tested tissues. (B) The major rBAT transcript (~2.5 kb) is also clearly visible only in kidney and intestine and is only slightly visible in liver on the original autoradiograph. A higher-molecular-weight transcript (~4.5 kb) is visible only in brain.

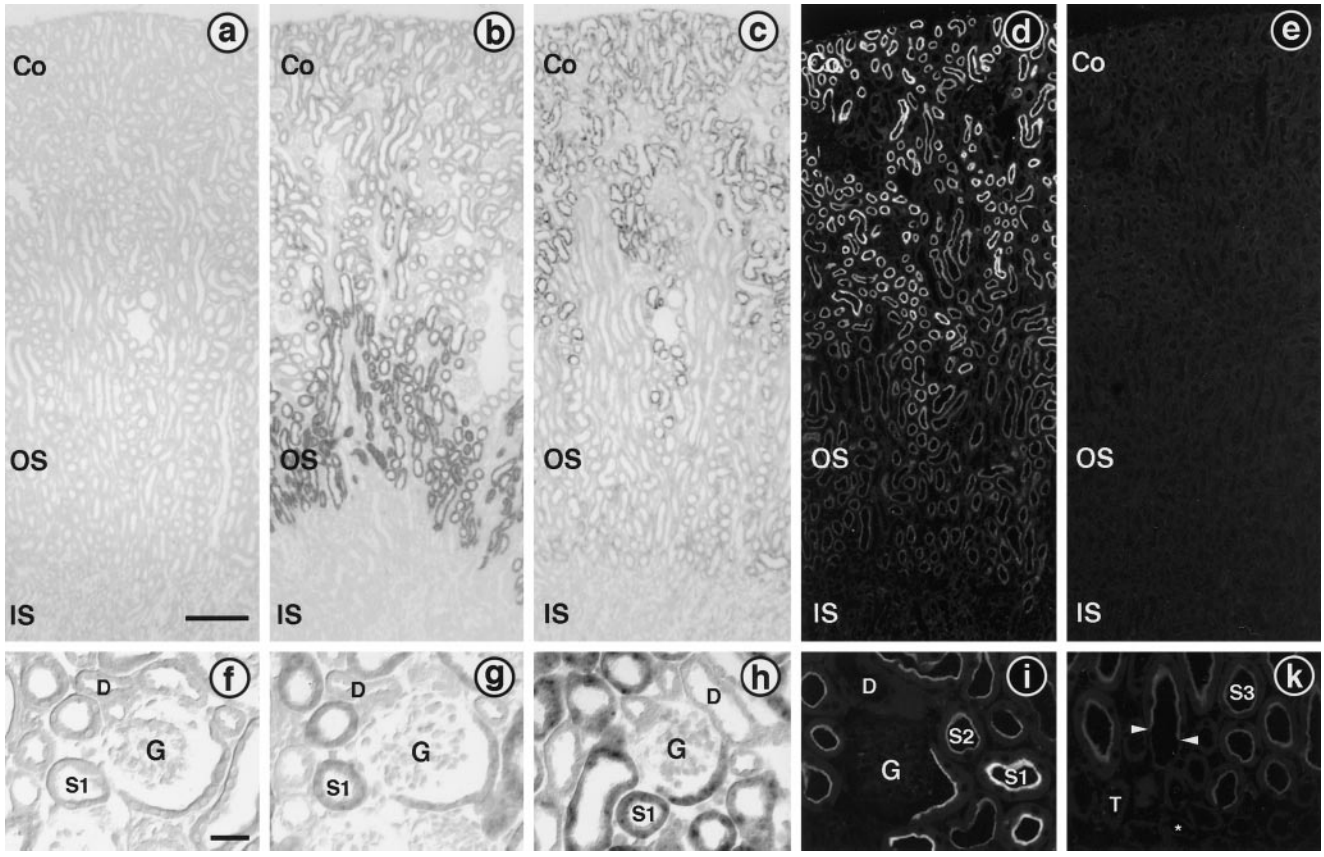

Figure 7. Distribution of rBAT and $b^{0,+}$AT in mouse kidney. Panels a–e show overviews of the cryosections (bar in a, 200 μm), and panels f–k show higher magnifications (bar in f, 50 μm). (a–c and f–h) In situ hybridizations. (b) Hybridization with a digoxigenin-labeled rBAT antisense riboprobe shows a strong signal in the outer stripe (OS) of the outer medulla, consistent with the previously reported preferential localization of rBAT mRNA in the S3 segments of proximal tubules. Weaker staining is also visible in proximal tubule profiles located in the renal cortex (Co), representing S1 and S2 segments. No staining is seen in the inner stripe (IS) of the outer medulla. (c) An inverse staining pattern is found in kidney sections hybridized with a $b^{0,+}$AT antisense riboprobe. Proximal tubules in the renal cortex are heavily stained, whereas only very weak staining is detectable in the medullary rays and in the outer stripe. However, the hybridization signal at these locations is higher than in the adjacent inner stripe and is clearly above the level obtained from sections hybridized with a digoxigenin-labeled $b^{0,+}$AT sense riboprobe (a). Higher magnifications of the renal cortex confirm the presence of rBAT mRNA (g) and $b^{0,+}$AT mRNA (h) in the S1 segments of proximal tubules, starting from the first S1 cells at the urinary pole of the glomerulus (G), whereas other cell types within the glomerulus and distal tubules (D) are unstained. No signal is detected in the corresponding control section hybridized with a rBAT sense riboprobe (f). (d, e, i, and k) Immunofluorescence. (d) Immunohistochemical detection of $b^{0,+}$AT at low magnification shows a bright immunofluorescent signal in proximal tubules within the renal cortex. Immunostaining, although at a lower intensity, is also visible in proximal tubules in the outer stripe. Preincubation of the antiserum with the antigenic peptide abolished the immunostaining completely (e). Higher magnifications of the cortex (i) and the outer medulla (k) show that $b^{0,+}$AT is exclusively present in the brush border at the luminal pole of proximal tubular cell from S1 (i) to S3 (k). Arrows in panel k point to the abrupt transition from an S3 segment (with the stained brush border) to a thin descending limb (unstained). Note the decreasing staining intensities from S1 to S2 to S3. The immunofluorescent staining of the brush border of the proximal tubule at the urinary pole of the glomerulus (G) is slightly weaker than farther downstream in S1. Cells within the glomerulus, cortical distal tubules (D) (i), medullary thick ascending limbs (T) (k), and thin descending limbs (asterisk) (k) are not labeled with the antiserum.

the brush border along the lumen of the entire proximal tubule from the beginning of S1 (panel i) to the end of S3 (panel k). The same immunohistochemical staining pattern was found in rat kidneys (data not shown). No staining was observed in glomeruli, distal tubules, or cells in the renal interstitium. All technical control experiments, such as hybridization with corresponding sense riboprobes (panel a and f) and immunohistochemistry after preincubation of the antiserum with the antigenic peptide (panel e) or with the preimmune serum (data not shown), were negative.

Localization of the Human Gene Encoding $hb^{0,+}$AT on Chromosome 19q

We performed fluorescent in situ hybridization of the $hb^{0,+}$AT cDNA on human metaphase chromosomes (data not shown). Positive hybridization signals were found consistently in the chromosomal region 19q, as expected for a candidate gene of cystinuria type III, the locus of which has been mapped to 19q13.1 (Bisceglia *et al.*, 1997; Wartenfeld *et al.*, 1997).

DISCUSSION

Differential Polarity of gpaATs Associating with 4F2hc or rBAT in Epithelia

The amino acid transporter $b^{0,+}$AT described in this study is a member of the recently characterized family of gpaATs. These transporters share high structural similarity, with 12 putative transmembrane domains and a conserved cysteine residue in the second putative extracellular loop that forms an intermolecular disulfide bridge with the so-called heavy chain (see model in Figure 2E) (Mastroberardino *et al.*, 1998; Pfeiffer *et al.*, 1998, 1999). The other light chains of the gpaAT family that have been described recently associate with 4F2hc, a type II glycoprotein required for their surface expression that displays a strict basolateral localization in renal and intestinal epithelia (Quackenbush *et al.*, 1986; Sordat, personal communication). These light chains exhibit differential localizations and specificities of amino acid transport. For instance, LAT1 is quite ubiquitous and accepts only neutral amino acids in a Na^+-independent manner. In contrast, y^+LAT1 is expressed prominently in kidney proximal tubule and small intestine at the basolateral membrane (associated with 4F2hc) and transports cationic amino acids in a Na^+-independent manner and neutral amino acids only in the presence of Na^+ (Pfeiffer *et al.*, 1999). Both LAT1 and y^+LAT1 have been shown to function as amino acid exchangers.

We and others have proposed that the amino acid transport system composed of y^+LAT1 and 4F2hc represents the basolateral exit pathway for cationic amino acids from kidney proximal tubule and small intestine cells (Torrents *et al.*, 1998; Pfeiffer *et al.*, 1999). Correspondingly, mutations in the gene encoding this member of the gpaAT family (SLC7A7) have been shown very recently to cause the genetic disease lysinuric protein intolerance (Borsani *et al.*, 1999; Torrents *et al.*, 1999). Interestingly, we have identified a second member of the gpaAT family that is also expressed in kidney proximal tubule and small intestine and is associated with 4F2hc at the basolateral membrane. Unlike the heterodimer formed by 4F2hc and y^+LAT, this second basolateral heterodimeric amino acid transporter (LAT2) displays a specificity of the L type similar to LAT1 (Rossier *et al.*, 2000).

In contrast to these gpaATs associated with 4F2hc and expressing their transport function at the basolateral membrane, we show here that $b^{0,+}$AT associates covalently with rBAT and is expressed in the apical brush border membrane. Importantly, these differentially polarized heterodimers are expressed mainly in the same kidney and small intestine cells and thus can participate in the same transepithelial amino acid transports. The rBAT-$b^{0,+}$AT complex is the high-affinity apical entry pathway for L-cystine and cationic amino acids (see also below), whereas 4F2hc-y^+LAT1 is the basolateral exit pathway for cationic amino acids and 4F2hc-LAT2 might play a role for the basolateral exit of some neutral amino acids such as cysteine, the reduction product of L-cystine (Torrents *et al.*, 1998, 1999; Borsani *et al.*, 1999; Pfeiffer *et al.*, 1999; Rossier *et al.*, 2000). Interestingly, the primary structure of $b^{0,+}$AT is equally similar to that of the LAT and y^+LAT members of the mammalian gpaAT family (~44% identity; see comparison with LAT1 and y^+LAT1 in Figure 1). This extent of identity is not much lower than that of 4F2hc-associated transporters of LAT and y^+LAT type (~49% identity). It will be interesting to localize the region(s) involved in the selective interaction of the gpaAT family members with either rBAT or 4F2hc. Because the mutation of the cysteine residues involved in intermolecular disulfide bond formation, in two different light chains (Pfeiffer *et al.*, 1998) and in 4F2hc (Estevez *et al.*, 1998; Pfeiffer *et al.*, 1998), has been shown to only slightly decrease the ability of the coexpressed heavy and light chains to form functional amino acid transporters at the surface of *Xenopus* oocytes, other regions of these proteins might play an important role in forming noncovalent interactions.

In conclusion, the interaction of the gpaAT family light chains with either 4F2hc or rBAT appears to determine their polarity of expression in epithelial cells. To date, it is not clear whether the heavy chains, besides determining the polarity of surface expression of the "catalytic" light chains, also participate in the transport and/or modulate its kinetics.

Function of $b^{0,+}$ATc as an L-Cystine Transporter

Earlier functional studies have indicated that the major part of L-cystine reabsorption in the kidney proximal tubule takes place in the S1 and S2 segments via a low-affinity and high-capacity system and that the final clearing of the tubular fluid from L-cystine takes place in the S3 segments via a high-affinity, low-capacity system corresponding to $b^{0,+}$-type transport (Palacin *et al.*, 1998, and references therein). In the present study, we show that $b^{0,+}$AT is expressed in the brush border membrane over the entire length of the proximal tubule, but at a much higher density in S1 and S2 than in S3. An earlier immunofluorescence study performed by others had shown that, in contrast to $b^{0,+}$AT, rBAT is expressed exclusively in the S3 segment of the rat kidney proximal tubule. Here we confirm in mouse kidney at the mRNA level the predominant expression of rBAT at the level of S3. However, we show that rBAT is also expressed, although at a lower level, in the earlier segments S1 and S2. Thus, the localization of the high-affinity L-cystine transport in S3 corresponds to the site of high rBAT and low $b^{0,+}$AT expression. The localization of the low-affinity, high-capacity L-cystine transport in S1 and S2 corresponds to that of high $b^{0,+}$AT and low rBAT expression.

We propose that the high-affinity, $b^{0,+}$-type L-cystine transport of the proximal kidney tubule S3 segment is mediated by the $b^{0,+}$AT-rBAT complex, in accordance with the localization data mentioned above and with the oocyte and M1 cell expression data, which demonstrate that the $b^{0,+}$AT-rBAT heterodimer functions as a high-affinity L-cystine transport system shared with cationic amino acids. To explain the discrepancy in rBAT and $b^{0,+}$AT expression levels along the proximal tubule, we propose two hypotheses that are compatible with the phenotype of rBAT defect (type I cystinuria: no amino aciduria in heterozygotes) and $b^{0,+}$AT defect (non-type I cystinuria: small amino aciduria in heterozygotes) (see references for cystinuria in INTRODUCTION). The first possibility is that rBAT is expressed in a large excess over $b^{0,+}$AT in the S3 segment and that all functional $b^{0,+}$ATs of the S1 and S2 segments are associated with rBAT as well. This complex could produce a low-affinity transport of L-cystine in the context of S1 and S2 cells, in contrast to the high-affinity transport observed in S3 cells and oocytes. Such differential transport kinetics could

be due to the presence in S1 and S2, or, alternatively, in S3 (and *Xenopus* oocytes), of another noncovalently associated protein that would modulate the transport function. The second possibility is that $b^{0,+}$AT is expressed in a large excess over rBAT in S1 and S2 and reaches the brush border membrane independent of association with rBAT. Because expression of functional surface transport requires the association of $b^{0,+}$AT with rBAT in oocytes and in transfected M1 cells (and in the S3 segment), one could postulate that surface expression in S1 and S2 requires the interaction with another apical membrane protein that is not expressed in S3 or in the cells used for exogenous expression mentioned above. In this putative complex with another membrane protein, $b^{0,+}$AT would express an amino acid transport with different kinetic properties, i.e., an L-cystine uptake with a lower apparent affinity, such as when it is associated with rBAT. However, this hypothesis remains quite speculative, in particular because database searches for rBAT-related proteins (candidates for association with $b^{0,+}$AT in S1 and S2) were unsuccessful.

It is important to mention that, concurrent with our study, several mutations have been identified by others in the genes encoding the $b^{0,+}$AT transporter (SLC7A9) of patients suffering from non-type I cystinuria (Palacin, personal communication). This confirms at the genetic level that $b^{0,+}$AT is involved in intestinal and renal L-cystine transport. This genetic information and the results of our biochemical, functional, and localization study complement each other to demonstrate that $b^{0,+}$AT, which is the product of the SLC7A9 gene, is the catalytic subunit of the hetero-oligomeric $b^{0,+}$ATc defective in cystinuria.

ACKNOWLEDGMENTS

The authors thank Brigitte Kaissling, in whose laboratory J.L. and D.L.-C. are working, for her support, Christian Gasser for the artwork, and Alexandra Albers for performing some of the fluorescent in situ hybridization experiments. The laboratory of F.V. is supported by Swiss National Science Foundation grant 31-49727.96. The project is also supported by grant 279-1-1996 from the Swiss Cancer League to L.C.K.

REFERENCES

Bertran, J., Werner, A., Chillaron, J., Nunes, V., Biber, J., Testar, X., Zorzano, A., Estivill, X., Murer, H., and Palacin, M. (1993). Expression cloning of a human renal cDNA that induces high affinity transport of L-cystine shared with dibasic amino acids in *Xenopus* oocytes. J. Biol. Chem. *268*, 14842–14849.

Bertran, J., Werner, A., Moore, M.L., Stange, G., Markovich, D., Biber, J., Testar, X., Zorzano, A., Palacin, M., and Murer, H. (1992). Expression cloning of a cDNA from rabbit kidney cortex that induces a single transport system for cystine and dibasic and neutral amino acids. Proc. Natl. Acad. Sci. USA *89*, 5601–5605.

Bisceglia, L., *et al.* (1997). Localization, by linkage analysis, of the cystinuria type III gene to chromosome 19q13.1. Am. J. Hum. Genet. *60*, 611–616.

Borsani, G., *et al.* (1999). SLC7A7, encoding a putative permease-related protein, is mutated in patients with lysinuric protein intolerance. Nat. Genet. *21*, 297–301.

Busch, A.E., Herzer, T., Waldegger, S., Schmidt, F., Palacin, M., Biber, J., Markovich, D., Murer, H., and Lang, F. (1994). Opposite directed currents induced by the transport of dibasic and neutral amino acids in *Xenopus* oocytes expressing the protein rBAT. J. Biol. Chem. *269*, 25581–25586.

Calonge, M.J., *et al.* (1994). Cystinuria caused by mutations in rBAT, a gene involved in the transport of cystine. Nat. Genet. *6*, 420–425.

Chillaron, J., *et al.* (1996). Obligatory amino acid exchange via systems $b^{0,+}$-like and y^+L-like: a tertiary active transport mechanism for renal reabsorption of cystine and dibasic amino acids. J. Biol. Chem. *271*, 17761–17770.

Coady, M.J., Jalal, F., Chen, X., Lemay, G., Berteloot, A., and Lapointe, J.Y. (1994). Electrogenic amino acid exchange via the rBAT transporter. FEBS Lett. *356*, 174–178.

Estevez, R., Camps, M., Rojas, A., Testar, X., Deves, R., Hediger, M., Zorzano, A., and Palacin, M. (1998). The amino acid transport system y^+L/4F2hc is a heteromultimeric complex. FASEB J. *12*, 1319–1329.

Foreman, J.W., Hwang, S.M., and Segal, S. (1980). Transport interactions of cystine and dibasic amino acids in isolated rat renal tubules. Metab. Clin. Exp. *29*, 53–61.

Furriols, M., Chillaron, J., Mora, C., Castello, A., Bertran, J., Camps, M., Testar, X., Vilaro, S., Zorzano, A., and Palacin, M. (1993). rBat, related to L-cysteine transport, is localized to the microvilli of proximal straight tubules, and its expression is regulated in kidney by development. J. Biol. Chem. *268*, 27060–27068.

Geering, K., Theulaz, I., Verrey, F., Häuptle, M.T., and Rossier, B.C. (1989). A role for the β-subunit in the expression of functional Na^+-K^+-ATPase in *Xenopus* oocytes. Am. J. Physiol. *257*, C851–C858.

Kanai, Y., Segawa, H., Miyamoto, K., Uchino, H., Takeda, E., and Endou, H. (1998). Expression cloning and characterization of a transporter for large neutral amino acids activated by the heavy chain of 4F2 antigen (CD98). J. Biol. Chem. *273*, 23629–23632.

Kanai, Y., Stelzner, M.G., Lee, W.S., Wells, R.G., Brown, D., and Hediger, M.A. (1992). Expression of mRNA (D2) encoding a protein involved in amino acid transport in S3 proximal tubule. Am. J. Physiol. *263*, F1087–F1092.

Loffing, J., Loffing-Cueni, D., Hegyi, I., Kaplan, M.R., Hebert, S.C., Le Hir, M., and Kaissling, B. (1996). Thiazide treatment of rats provokes apoptosis in distal tubule cells. Kidney Int. *50*, 1180–1190.

Mannion, B.A., Kolesnikova, T.V., Lin, S.H., Wang, S., Thompson, N.L., and Hemler, M.E. (1998). The light chain of CD98 is identified as E16/TA1 protein. J. Biol. Chem. *273*, 33127–33129.

Mao, Q., Schunk, T., Gerber, B., and Erni, B. (1995). A string of enzymes, purification and characterization of a fusion protein comprising the four subunits of the glucose phosphotransferase system of *Escherichia coli*. J. Biol. Chem. *270*, 18295–18300.

Mastroberardino, L., Spindler, B., Pfeiffer, R., Skelly, P.J., Loffing, J., Shoemaker, C.B., and Verrey, F. (1998). Amino acid transport by heterodimers of 4F2hc/CD98 and members of a permease family. Nature *395*, 288–291.

Mosckovitz, R., Udenfriend, S., Felix, A., Heimer, E., and Tate, S.S. (1994). Membrane topology of the rat kidney neutral and basic amino acid transporter. FASEB J. *8*, 1069–1074.

Nakamura, E., Sato, M., Yang, H., Miyagawa, F., Harasaki, M., Tomita, K., Matsuoka, S., Noma, A., Iwai, K., and Minato, N. (1999). 4F2 (CD98) heavy chain is associated covalently with an amino acid transporter and controls intracellular trafficking and membrane topology of 4F2 heterodimer. J. Biol. Chem. *274*, 3009–3016.

Palacin, M., Chillaron, J., and Mora, C. (1996). Role of the $b^{0,+}$-like amino acid-transport system in the renal reabsorption of cystine and dibasic amino acids. Biochem. Soc. Trans. *24*, 856–863.

Palacin, M., Estevez, R., Bertran, J., and Zorzano, A. (1998). Molecular biology of mammalian plasma membrane amino acid transporters. Physiol. Rev. *78*, 969–1054.

Pfeiffer, R., Rossier, G., Spindler, B., Meier, C., Kühn, L.C., and Verrey, F. (1999). Amino acid transport of y^+L-type by heterodimers of 4F2hc/CD98 and members of the glycoprotein-associated amino acid transporter family. EMBO J. *18*, 49–57.

Pfeiffer, R., Spindler, B., Loffing, J., Skelly, P., Shoemaker, C., and Verrey, F. (1998). Functional heterodimeric amino acid transporters lacking cysteine residues involved in disulfide bond. FEBS Lett. *439*, 157–162.

Pras, E., Kochba, I., Lubetzky, A., Pras, M., Sidi, Y., and Kastner, D. (1998). Biochemical and clinical studies in Libyan Jewish cystinuria patients and their relatives. Am. J. Med. Genet. *80*, 173–176.

Prasad, P.D., Wang, H., Huang, W., Kekuda, R., Rajan, D.P., Leibach, F.H., and Ganapathy, V. (1999). Human LAT1, a subunit of system L amino acid transporter: molecular cloning and transport function. Biochem. Biophys. Res. Commun. *255*, 283–288.

Puoti, A., May, A., Rossier, B.C., and Horisberger, J.D. (1997). Novel isoforms of the β and γ subunits of the *Xenopus laevis* Na channel provide information about the amiloride binding site and extracellular sodium sensing. Proc. Natl. Acad. Sci. USA *94*, 5949–5954.

Quackenbush, E.J., Gougos, A., Baumal, R., and Letarte, M. (1986). Differential localization within human kidney of five membrane proteins expressed on acute lymphoblastic leukemia cells. J. Immunol. *136*, 118–124.

Riahi-Esfahani, S., Jessen, H., and Roigaard, H. (1995). Comparative study of the uptake of L-cysteine and L-cystine in the renal proximal tubule. Amino Acids *8*, 247–264.

Rosenberg, L.E., Downing, S., Durant, J.L., and Segal, S. (1966). Cystinuria: biochemical evidence for three genetically distinct diseases. J. Clin. Invest. *45*, 365–371.

Rossier, G., Meier, C., Bauch, C., Summa, V., Sordat, B., Verrey, F., and Kühn, L.C. (2000). LAT2: a new basolateral 4F2hc/CD98-associated amino acid transporter of kidney and intestine. J. Biol. Chem. (*in press*).

Schafer, J.A., and Watkins, M.L. (1984). Transport of L-cystine in isolated perfused proximal straight tubules. Pfluegers Arch. *401*, 143–151.

Silbernagl, S. (1988). The renal handling of amino acids and oligopeptides. Physiol. Rev. *68*, 911–1007.

Tate, S.S., Yan, N., and Udenfriend, S. (1992). Expression cloning of a Na^+-independent neutral amino acid transporter from rat kidney. Proc. Natl. Acad. Sci. USA *89*, 1–5.

Torrents, D., Estevez, R., Pineda, M., Fernandez, E., Lloberas, J., Shi, Y., Zorzano, A., and Palacin, M. (1998). Identification and characterization of a membrane protein (y^+L amino acid transporter-1) that associates with 4F2hc to encode the amino acid transport activity y^+L: a candidate gene for lysinuric protein intolerance. J. Biol. Chem. *273*, 32437–32445.

Torrents, D., *et al.* (1999). Identification of SLC7A7, encoding y^+LAT-1, as the lysinuric protein intolerance gene. Nat. Genet. *21*, 293–296.

Van Winkle, L.J. (1988). Amino acid transport in developing animal oocytes and early conceptuses. Biochim. Biophys. Acta *947*, 173–208.

Wang, Y., and Tate, S.S. (1995). Oligomeric structure of a renal cystine transporter: implications in cystinuria. FEBS Lett. *368*, 389–392.

Wartenfeld, R., Golomb, E., Katz, G., Bale, S.J., Goldman, B., Pras, M., Kastner, D.L., and Pras, E. (1997). Molecular analysis of cystinuria in Libyan Jews: exclusion of the SLC3A1 gene and mapping of a new locus on 19q. Am. J. Hum. Genet. *60*, 617–624.

Wells, R.G., and Hediger, M.A. (1992). Cloning of a rat kidney cDNA that stimulates dibasic and neutral amino acid transport and has sequence similarity to glucosidases. Proc. Natl. Acad. Sci. USA *89*, 5596–5600.

Yan, N., Mosckovitz, R., Udenfriend, S., and Tate, S.S. (1992). Distribution of mRNA of a Na^+-independent neutral amino acid transporter cloned from rat kidney and its expression in mammalian tissues and *Xenopus laevis* oocytes. Proc. Natl. Acad. Sci. USA *89*, 9982–9985.